Academic Journal of Science and Technology
ISSN: 2771-3032 | Vol. 8, No. 2, 2023

Stability Analysis of Surrounding Rock in Deep Underground Engineering Under Fluid-solid Interaction

Haikun Shan[1], Xiaohu Yuan[2]

[1]School of Civil Engineering, Henan University of Technology, Henan 454000, China
[2]China State Construction Railway Investment &Engineering Group Ltd, Beijing 102600, China

Abstract: The geological environment of deep rock masses is extreme and complex, characterized by typical deep geological features such as high geostress, high permeation water pressure, and high geotemperature. Geological disasters like water and mud inrush, high-intensity rock bursts, and large-volume collapses occur frequently in engineering construction, presenting more complex mechanisms of disaster than shallower rock masses and severely impacting the construction and operational safety of deep underground projects. Utilizing three-dimensional numerical simulation methods, this study investigated the deformation, stress, and plastic zone characteristics of surrounding rock under multi-field coupling conditions during the construction of deep caverns, revealing the stability influencing factors of deep caverns under multi-field coupling. A funnel-shaped precipitation area forms near the excavation surface of the cavern, gradually expanding as the initial pore water pressure increases. The concentration of seepage vectors in the sidewalls and arch feet continues to increase, with local seepage rates reaching 5.1×10^-6. The cavern's crown and sidewalls are particularly sensitive to changes in pore water pressure, with the maximum tensile stress appearing 1 m and 3 m axially along the sidewalls of the cavern. The plastic zone experiences its greatest increase at a water pressure of 4 MPa.

Keywords: Deep Engineering; Multi-field Coupling; Surrounding Rock; Stability; Numerical Simulation.

1. Introduction

Deep underground engineering projects, situated in environments characterized by high geostress, high geotemperature, and high permeation water pressure (the "three highs"), are subject to intense geological structural activities. These conditions, exacerbated by large-scale excavation and rapid unloading disturbances, frequently lead to instability in cavern surrounding rocks, triggering a series of deep engineering disasters such as intense rock bursts, continuous large deformations, and large-volume collapses. These incidents result in significant casualties, project delays, and economic losses, severely hampering the safe construction and normal operation of deep underground projects. The stability analysis and disaster prevention of underground projects under these unique deep conditions have become major issues concerning national property, people's lives, and national defense security, and are currently a focal point in the field of underground engineering research worldwide. Due to the complexity of deep engineering environments, the stability theories and related technical systems developed for shallower projects are partially or severely ineffective when applied in deep environments, posing unprecedented challenges to the stability of deep underground projects. Therefore, conducting research on the stability evaluation and optimized design of underground engineering under multi-field coupling in deep environments aligns with the significant demands of national resource and technological development and holds vital engineering value and strategic significance for ensuring construction safety in underground projects.

During the construction phase of deep underground projects, fluid-solid coupling primarily manifests as changes in the original geostress field due to construction disturbances. These inevitably lead to alterations in the effective stress within the rock and soil bodies, affecting the distribution of groundwater and, in turn, causing a redistribution of the seepage field within the rock and soil bodies. This change in the seepage field alters the stress field, thus creating a fluid-solid coupling effect in underground engineering. In 1923, Terzaghi proposed the principle of effective stress, laying the theoretical foundation for stress-seepage coupling in rock and soil media with his one-dimensional consolidation equation for homogeneous saturated soil. Biot expanded this one-dimensional consolidation theory into a more comprehensive three-dimensional consolidation theory for rock and soil media, providing analytical solutions and examples for classic problems. Huang Tao et al. proposed a mathematical model for predicting the water inrush volume of fractured surrounding rock tunnels under stress and seepage coupling and validated it with a three-dimensional tunnel model based on actual projects. Li Zongli et al. achieved fluid-solid coupling by applying seepage force as a volumetric force in the stress field, deriving analytical expressions for the elastic displacement and stress of tunnels under coupling, and using the Mohr-Coulomb yield criterion to solve for the plastic radius and stress of tunnels. Their comparative analysis of examples considering coupling effects and those not showed that considering coupling effects increases the plastic radius and wall displacement of tunnel surrounding rocks.

Studies on the distribution and variation patterns of the temperature field in the surrounding rocks of caverns under different original rock temperature conditions, particularly considering ventilation and heat dissipation, are relatively scarce. Therefore, this paper uses numerical simulation methods to study the temperature distribution characteristics of the surrounding rocks of deep underground caverns during the construction phase under different original rock temperatures, based on a systematic study of high-

geotemperature engineering conditions at home and abroad. The research on the impact of different rock body temperatures on the internal temperature distribution of the surrounding rocks and their deformation characteristics holds practical significance for effectively addressing high-temperature thermal damage and ensuring the safety and stability of cavern surrounding rocks.

2. Stability Analysis of Surrounding Rock of Deep Underground Engineering Under Fluid-solid Interaction

2.1. Numerical models and parameters

In the three-dimensional model of the deep underground engineering cavern, the clear distance between the upper arch crown and the lower arch bottom is set at 5.3 meters, with a left-right clear spacing of 6 meters. The model extends four times the cavern diameter on both left and right sides, and four times the diameter below, with a burial depth of 1200 meters. The overall model measures 50 meters in width, 50 meters in height, and 10 meters in depth, as illustrated in Figure 1. The mechanical boundary conditions of the model are defined as follows: a pressure of 30 MPa is applied at the top, normal constraints are imposed on both left and right sides as well as on the front and rear, and the bottom surface is fixed.

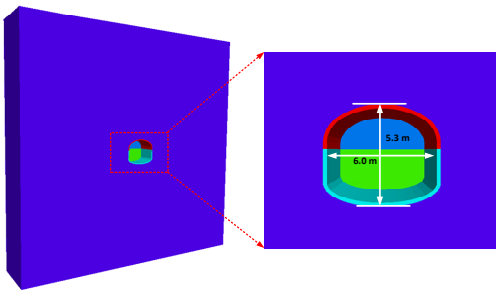

Figure 1. Numerical model

During the numerical calculation process, the surrounding rock of the cavern is considered as an isotropic Mohr-Coulomb ideal elasto-plastic material. The shotcrete layer is simulated using solid elements and treated as an isotropic linear elastic material, with a layer thickness of 20 cm. Anchor bolts are modeled using cable structural elements, with a diameter of 10 mm and full-length anchorage. The physical and mechanical parameters of the cavern's surrounding rock, the initial support shotcrete layer, and the anchor bolts are presented in Tables 1 and 2.

Table 1. Mechanical parameters of surrounding rock

Material type	Density (kg/m^3)	Bulk modulus (GPa)	shear modulus (GPa)	Cohesion (MPa)	internal friction angle (°)	permeability coefficient (m*d-1)	porosity
Initial spraying of surrounding rock	2500	5.38	3.36	7.8	24.5	9.8×10-12	0.21
Initial spraying of surrounding rock	2000	20.7	12.6	——	——	——	——

Table 2. Mechanical parameters of bolt

elastic modulus (GPa)	cross-section area (m2)	slurry cohesion (MPa)	friction angle of slurry (°)	cement slurry stiffness (GPa)	perimeter of cement slurry outer ring (m)	tensile strength (N/mm²)
45	3.14×10-4	0.8	30	0.7	1.0	300

2.2. Boundary constraints

To study the changes in the seepage field, displacement, stress, and plastic zone during the construction of deep underground caverns under different initial pore water pressure conditions, the model's top pore water pressure is set at three levels: 0.5 MPa, 1 MPa, 2 MPa, and 4 MPa, for comparative analysis. The permeability boundary conditions are established with fixed hydraulic pressure applied to the top surface, while the left, right, and bottom boundaries are assumed to be impermeable. The excavation boundary of the cavern is set as a free seepage boundary, allowing water to freely infiltrate into the interior of the cavern, with the fixed pore water pressure set to 0. Additionally, each excavation advancement of the cavern is set at 2 meters, followed by a set duration of fluid-solid coupling calculation after each advancement with the current advancement's cavern surface fixed pore water pressure set to 0, and then proceeding with anchor shotcrete support. These steps are repeated in sequence to complete three phases of excavation for the deep underground cavern.

3. Multivariate Information Characteristics of Deep Cavern Surrounding Rock Under Multi-field Coupling

3.1. Analysis of the displacement of surrounding rock under different pore water pressures

The deformation of surrounding rock during the construction of deep underground engineering projects directly reflects the disturbance level to the rock mass caused by cavern construction. This paper primarily analyzes the deformation patterns of surrounding rock near the cavern due to excavation under different initial pore water pressure conditions.

The vertical displacement cloud diagrams of the surrounding rock at the 3-meter section of the cavern under different initial pore water pressures are shown in Figure 2. As can be seen from the diagram, the vertical displacement changes in the surrounding rock of the cavern are mainly

manifested as settlement at the arch crown and uplift at the arch bottom. Both the settlement displacement at the arch crown and the uplift displacement at the arch bottom increase progressively with the increase in initial pore water pressure.

The maximum settlement deformation under each pore water pressure occurs at the cavern arch crown, with settlements of 9.62 cm, 9.81 cm, 10.01 cm, and 10.65 cm, respectively; the maximum uplift occurs at the cavern arch bottom, with displacements of 10.10 cm, 10.41 cm, 10.75 cm, and 11.12 cm, respectively. The growth magnitude of the arch crown displacement increases with the increase in the initial pore water pressure. When the pore water pressure increases from 0.5 MPa to 1 MPa, the displacement values for both the arch crown settlement and arch bottom uplift show only a minor increase. However, when the pore water pressure increases from 2 MPa to 4 MPa, there is a significant change in the settlement displacement at the arch crown, with a notable increase in displacement amount. The uplift at the arch bottom shows a nearly linear increase with increasing pore water pressure, and the uplift displacement at the arch bottom under different pore water pressures is consistently greater than the settlement displacement at the arch crown.

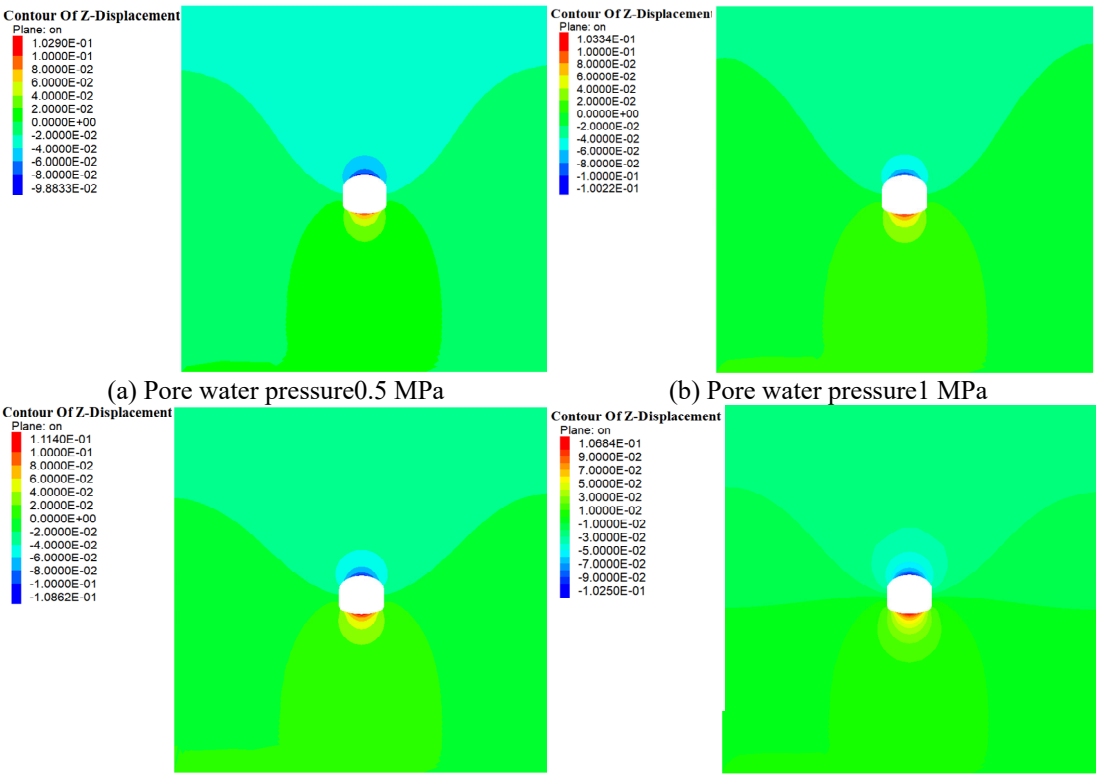

(a) Pore water pressure0.5 MPa (b) Pore water pressure1 MPa

(c) Pore water pressure2 MPa (d) Pore water pressure4 MPa

Figure 2. Vertical displacement clouds at different pore water pressures

3.2. Stress analysis of surrounding rock under different pore water pressures

To analyze the impact of changes in the seepage field on the stress field of the surrounding rock in the cavern, the maximum stress cloud diagram and the minimum principal stress cloud diagram of the surrounding rock at the 3-meter section of a deep underground cavern under different initial pore water pressure conditions are shown in Figure 3. From the diagrams, it is evident that regardless of the initial pore water pressure, after the excavation progresses 2 meters into the cavern, the surrounding rock moves slightly towards the free face. This uneven deformation causes a redistribution of the stress field, leading to uneven stress concentration on the cavern surface and consequently, causing damage to the surrounding rock. The maximum principal stress field around the excavation face undergoes significant changes, with noticeable stress variations within a 5-6 meter range above and below the arch crown and bottom. The stress change area on the sides of the sidewalls is confined to a 2-3 meter range, significantly smaller than the stress-affected area of the arch crown and bottom. Figure 3 shows that the maximum principal stress in the surrounding rock of the cavern's first excavation step is mainly composed of stress concentration bands and stress reduction areas near the voids. This region is particularly evident at the center of the arch crown and bottom and at the sidewalls, with the maximum principal stress values of the surrounding rock on the cavern surface mainly concentrated between -22.5 MPa and -2.5 MPa. The stress concentration area is primarily located at the intersections of the sidewalls and the arch crown and bottom, with the degree of stress concentration increasing as the initial pore water pressure increases. The maximum principal stress values at the center of the arch crown, bottom, and sidewalls are significantly lower than those in the stress concentration areas, with little variation in maximum principal stress values under different pore water pressures. Under different pore water pressure conditions, the maximum principal stress on the excavation face exhibits varying degrees of tensile stress concentration, which increases as the pore water pressure increases, indicating that the potential damage extent of the workface increases with increasing pore water pressure. As the distance from the excavation workface increases, the maximum principal stress gradually increases to positive values, transitioning from tensile to compressive stress.

When the excavation progress reaches 4 meters, under the combined influence of the stress field and seepage field, positive values of maximum principal stress occur in the

surrounding rock of the cavern sidewalls at 1 meter and 3 meters along the cavern axis. The surrounding rock stress is tensile, which is extremely disadvantageous for the stability of the surrounding rock in a cavern, as rock and soil materials have far greater compressive than tensile strength. Therefore, the stability of this part of the surrounding rock should be given attention, and reinforcement treatment should be considered when necessary. The degree of concentration of the maximum principal stress at the arch shoulders and feet increases with the excavation progress. Under different initial pore water pressure conditions, the range of the maximum principal stress field affected by excavation disturbances after the second excavation step increases to varying degrees compared to the first excavation, and the degree of stress concentration in different parts of the cavern also significantly increases. After stabilizing the excavation progress at 4 meters, the maximum principal stress values in different parts behind the shotcrete layer of the cavern reveal that the maximum principal stress at the arch shoulders and feet is significantly higher than at the arch crown and bottom. This is mainly because the arch shoulders and feet not only bear the stress generated by the deformation of the upper surrounding rock but also the stress transmitted from the support structure, leading to a significant increase in the maximum principal stress compared to the arch crown and bottom.

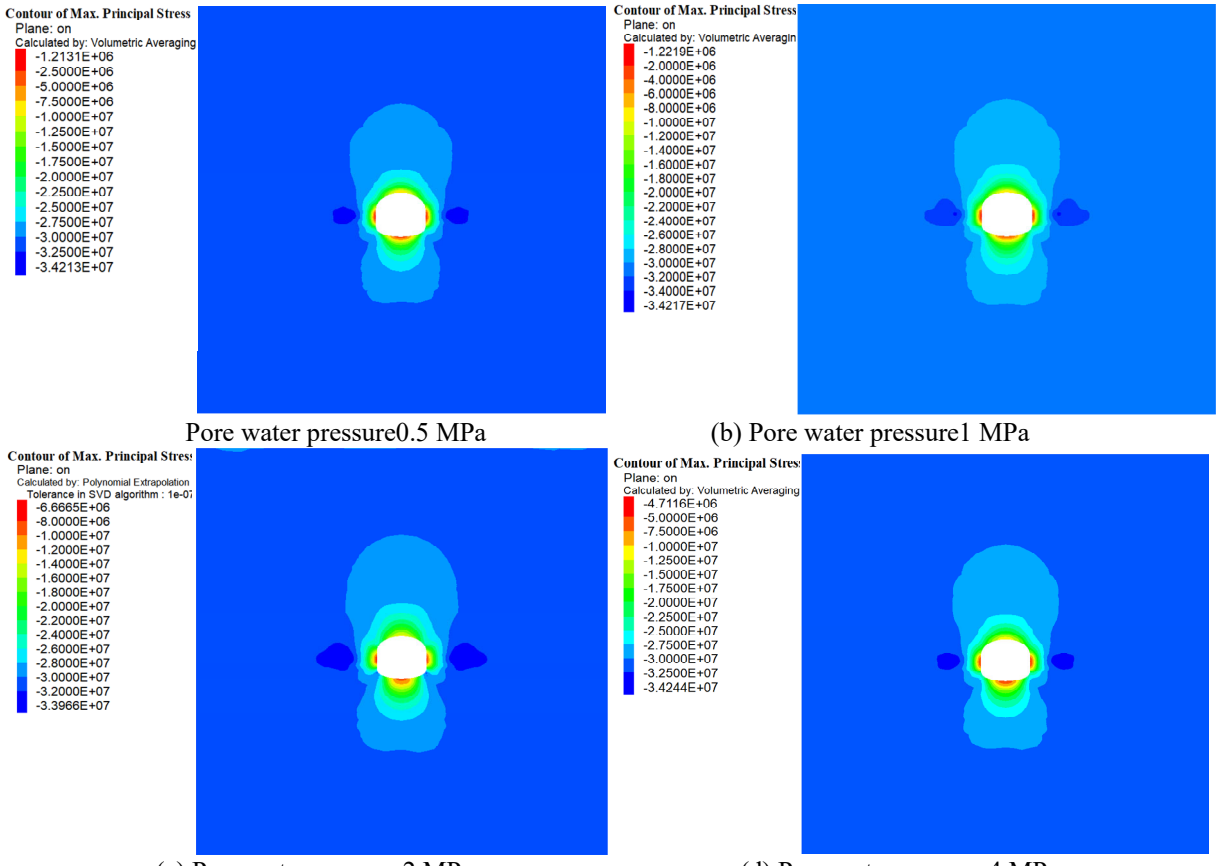

Pore water pressure0.5 MPa (b) Pore water pressure1 MPa

(c) Pore water pressure2 MPa (d) Pore water pressure4 MPa

Figure 3. Maximum principal stress cloud

3.3. Analysis of the plastic zone of surrounding rock under different pore water pressures

Figure 4 illustrates the distribution of the plastic zone in the surrounding rock under different initial pore water pressures, considering the effect of fluid-solid coupling. A comparison of Figures 4(a) to 4(d) reveals that as the initial pore water pressure of the surrounding rock increases, the impact range of the plastic zone gradually expands. The distribution of the plastic zone in the surrounding rock under different initial pore water pressures is similar. With lower pore water pressures (Figures 4(a) and 4(b)), small-scale plastic failure occurs at the arch shoulders and feet of the cavern, followed by the sidewalls, while the arch crown has almost no effective plastic zone. The surrounding rock mainly undergoes shear yield failure, with the sidewalls experiencing minor shear failure and a small range of tensile yield failure in the rock mass. When the initial pore water pressure increases to 2 MPa and 4 MPa, the increase in the plastic zone becomes more pronounced, with a tendency to develop deeper into the surrounding rock. In addition to the aforementioned failure characteristics under lower pore water pressure conditions, tensile yield failure starts to appear at the arch bottom and crown of the cavern. As the pore water pressure increases, the extent of damage to the cavern also significantly increases. Therefore, in the construction of underground projects under high pore water pressure environments, it is necessary to timely increase the shear strength of the surrounding rock through measures such as advance grouting and anchor bolt installation to improve the rock mass quality, thus preventing the excessive development of the plastic zone in the surrounding rock during construction and its evolution into a geological engineering disaster.

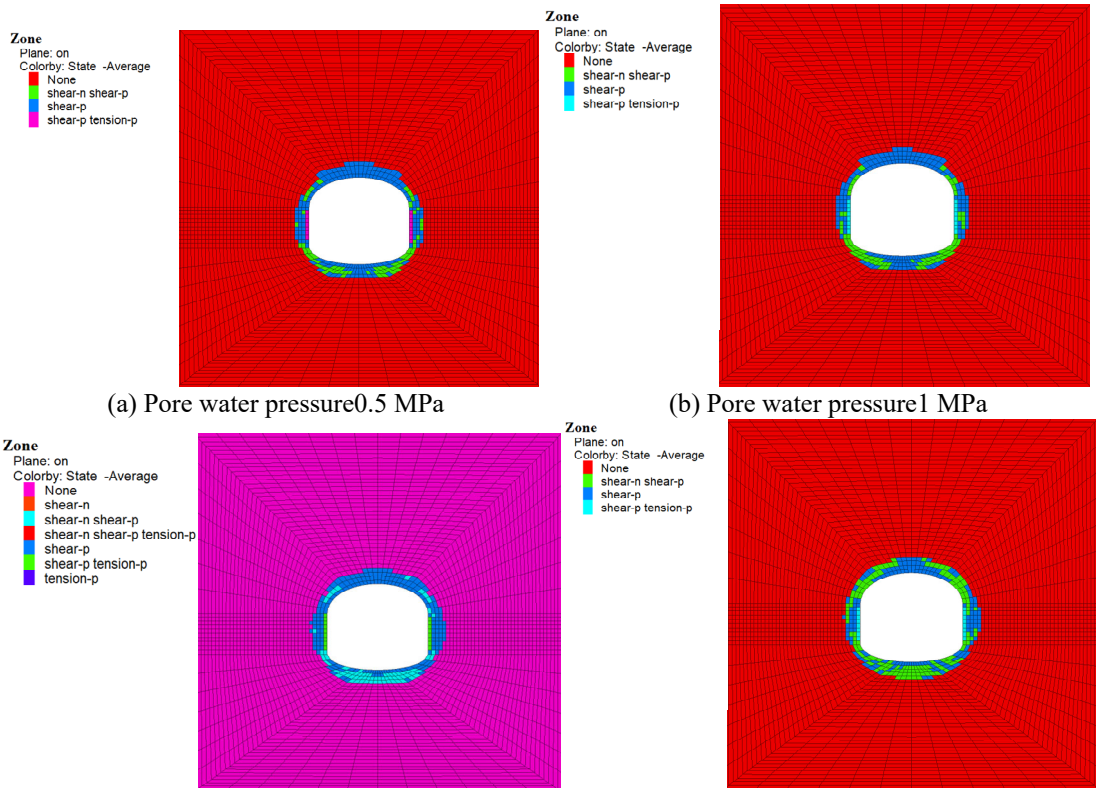

(a) Pore water pressure0.5 MPa (b) Pore water pressure1 MPa

(c) Pore water pressure2 MPa (d) Pore water pressure4 MPa

Figure 4. Distribution of plastic zones in the surrounding rock under different working conditions

4. Conclusion

This chapter conducts simulation studies on cavern excavation construction under different initial pore water pressure conditions. Through an in-depth analysis of the post-excavation seepage field distribution, the stress on the surrounding rock, and the distribution of the surrounding rock and plastic zone of the cavern, the following conclusions are drawn:

(1) The increase in arch crown displacement of the cavern amplifies with the increase in initial pore water pressure, and the uplift at the arch bottom shows a nearly linear increase with increasing pore water pressure. During the cavern excavation process, the front of the excavation workface experiences minor displacement due to excavation disturbances. When excavating to the monitoring cross-section, both horizontal and vertical displacements of the surrounding rock show a linear increase, with a slight growth as the excavation face continues to advance.

(2) Under different initial pore water pressures, the stress in the surrounding rock of the cavern's first excavation step mainly consists of stress concentration bands and stress reduction areas near voids, with the degree of stress concentration increasing as the initial pore water pressure increases. When the excavation progress reaches 4 meters, tensile stress occurs in the maximum principal stress of the surrounding rock at 1 meter and 3 meters along the cavern axis.

(3) As the initial pore water pressure of the surrounding rock increases, the impact range of the plastic zone gradually expands. With lower pore water pressures, small-scale plastic failure occurs at the arch shoulders and feet of the cavern. When the initial pore water pressure increases to 2 MPa and 4 MPa, the increase in the plastic zone becomes more pronounced, with a tendency to develop deeper into the surrounding rock.

References

[1] Liang Weizhang, Zhao Guoyan. Research Progress on Rockburst Risk Prevention and Control Technology in Deep Hard Rock Mines [J]. Rock and Soil Mechanics. 2022, 43(S2): 454-468.

[2] Terzaghi K. Theoretical Soil Mechanics[M]. 2007, i - xvii.

[3] Biot M A. General Theory of Three-Dimensional Consolidation[J]. Journal of Applied Physics. 1941, 12: 155-164.

[4] Biot M A. Theory of Elasticity and Consolidation for a Porous Anisotropic Solid[J]. Journal of Applied Physics. 1955, 26(2): 182-185.

[5] Biot M A. General solutions of equations of elasticity and consolidation for a porous material[J]. J.appl.phys. 1956, 23: 91-96.

[6] Huang Tao, Yang Lizhong. Research on Predicting Water Inrush in Fractured Surrounding Rock Tunnels under Seepage and Stress Coupling Environment [J]. Journal of the China Railway Society. 1999(06): 75-80.

[7] Li Zongli, Ren Qingwen, Wang Yahong. Elastic-Plastic Solution for Deeply Buried Circular Tunnels Considering the Influence of Seepage Field [J]. Chinese Journal of Rock Mechanics and Engineering. 2004, 23(8): 1291-1295.